

SPECTRAL APPROACH TO D-BAR PROBLEMS

CHRISTIAN KLEIN AND KEN MCLAUGHLIN

ABSTRACT. We present the first numerical approach to D-bar problems having spectral convergence for real analytic rapidly decreasing potentials. The proposed method starts from a formulation of the problem in terms of an integral equation which is solved with Fourier techniques. The singular integrand is regularized analytically. The resulting integral equation is approximated via a discrete system which is solved with Krylov methods. As an example, the D-bar problem for the Davey-Stewartson II equations is solved. The result is used to test direct numerical solutions of the PDE.

1. INTRODUCTION

It is the purpose of this paper to present an efficient numerical approach to solve D-Bar equations for a complex valued unknown $\psi = \psi(x, y)$, i.e.,

$$(1) \quad \bar{\partial}\psi = \frac{1}{2}Q(x, y)\bar{\psi}.$$

In (1), one has $(x, y) \in \mathbb{R}^2$, and we often use $z = x + iy$, as well as $\bar{\partial} = \frac{1}{2} \left(\frac{\partial}{\partial x} + i \frac{\partial}{\partial y} \right)$. The function Q is a given “potential” which we assume to be a function in the Schwartz class $\mathcal{S}(\mathbb{R}^2)$ of rapidly decreasing smooth functions in the plane.

This equation appears in a number of different areas of analysis and applied mathematics, most prominently in Electrical Impedance Tomography which is of enormous importance in medical imaging, in the solution of completely integrable 2 + 1 dimensional partial differential equations (PDEs), as well as in two-dimensional orthogonal polynomials and random matrix theory (see below for details and references).

In this paper we will primarily be interested in *Complex Geometrical Optics* (CGO) solutions of (1) defined by the normalization at infinity,

$$(2) \quad \psi e^{-kz} = 1 + \mathcal{O}\left(\frac{1}{|z|}\right),$$

where $k \in \mathbb{C}$ is an auxiliary parameter.

In order to make use of the Fourier transform, we express ψ in terms of m which tends to 0 as $|z| \rightarrow \infty$:

$$(3) \quad m = \psi e^{-kz} - 1.$$

This new quantity now solves

$$(4) \quad \bar{\partial}m = \frac{1}{2}e^{\bar{k}z - kz}Q(\bar{m} + 1).$$

Taking the Fourier transform defined via

$$(5) \quad \mathcal{F}(f) = \hat{f}(\xi) = \frac{1}{2\pi} \int_{\mathbb{R}^2} f(x, y) e^{-i\xi_1 x - i\xi_2 y} dx dy, \quad \mathcal{F}^{-1}(\hat{f}) = f(x, y) = \frac{1}{2\pi} \int_{\mathbb{R}^2} \hat{f}(\xi_1, \xi_2) e^{i\xi_1 x + i\xi_2 y} d\xi,$$

we find that (formally) \hat{m} solves

$$(6) \quad i\xi \hat{m} = \mathcal{F} \left\{ Q e^{\bar{k}z - kz} (\bar{m}) \right\} + \mathcal{F} \left\{ Q e^{\bar{k}z - kz} \right\}.$$

It turns out to be convenient for the numerical approach to write the equation in terms of

$$(7) \quad S(\xi) = \xi \hat{m}(\xi),$$

Date: August 11, 2015.

Key words and phrases. D-bar problems, Fourier spectral method, Davey-Stewartson equations.

since \hat{m} is unbounded for $|\xi| \rightarrow 0$, whereas S is not. Thus the fundamental equation of study is

$$(8) \quad S(\xi) = -i\mathcal{F} \left\{ Qe^{\bar{k}z-kz} \left(\overline{\mathcal{F}^{-1} \left(\frac{1}{\xi} S(\xi) \right)} \right) \right\} - i\mathcal{F} \left\{ Qe^{\bar{k}z-kz} \right\} .$$

A brief gaze at (8) reveals the primary obstacle for a numerical approach: the division by ξ , although a weak singularity in two dimensions, needs to be addressed.

The approach we have developed to overcome this obstacle is to re-write the equation in a manner which peels off the singular behavior. The offending term appearing in (8) is re-written as follows:

$$\mathcal{F}^{-1} \left(\frac{1}{\xi} S(\xi) \right) = \mathcal{F}^{-1} \left(\frac{1}{\xi} (S(\xi) - G(\xi)) \right) + \mathcal{F}^{-1} \left(\frac{1}{\xi} G(\xi) \right) ,$$

and the function G is chosen so that the following conditions are met:

- The first term above is smooth at $\xi = 0$ (to machine precision) and vanishing (again to machine precision) at the boundary of the computational domain.
- The second piece, containing all the singular terms, is evaluated via *explicit analytical calculation*.

Below we choose the function G to essentially contain the "anti-holomorphic part" of the function S , or more precisely a truncated Taylor series representing the anti-holomorphic part of S , multiplied by a Gaussian.

For the numerical evaluation, the Schwartz functions are treated as essentially periodic (the computational domain is chosen large enough that the studied functions and their derivatives vanish to within numerical precision at the boundaries of the domain). The Fourier series is approximated numerically via a discrete Fourier series, computed via a Fast Fourier Transform (FFT). Thus the integral equation (8) is approximated via a system of linear equations for a matrix S (denoted with the same symbol in an abuse of notation) of finite dimension.

In many applications, including the Davey-Stewartson equation, one often needs the solution for many values of the auxiliary parameter k . The approach briefly outlined above works for small values of $|k|$, and the ensuing system can be solved iteratively via GMRES [22].

We show, however, that for large values of k , this first approach does not work adequately, because the support of the desired solution is no longer distant from the boundary of the computational domain (for the Fourier transform variable). We develop a re-formulation of the (Fourier transformed) $\bar{\partial}$ equation based on the support properties of the solution for large k , which yields a once iterated variant of (8) and handles disparate support issues via careful shifting within the computational domain. Remarkably, this new equation is equivalent (up to a Fourier transform) of the iterated system of equations which Perry studies in ([26]), and in fact can be effectively used for *all values of k* .

We study the convergence of the method for concrete examples and show that the numerical approach has *spectral convergence*, i.e., that the numerical error decreases exponentially for smooth functions. The approach is then applied to the D-bar problem of the Davey-Stewartson (DS) II equation, and the resulting solution is compared to a direct numerical solution of DS II as in [13].

The paper is organized as follows: In section 2 we briefly summarize some of the main applications of the D-bar problem, and previous numerical approaches to its solution. In section 3 we present a short review on the existence theory for equation (8). In section 4 we discuss the numerical implementation of a regularization approach for $|\xi| \rightarrow 0$ of the integrand in (8). In section 5 we derive a once iterated version of equation (8) which is shown to be convenient for the construction of CGO solutions to D-bar problems, and use the approach of section 4 (along with careful shifting) for this equation. This approach is applied to the D-bar problem for the DS II system as an example in section 6. The obtained solution is compared to a DS II solution for the same initial data via a direct numerical integration of DS II. We add some concluding remarks in section 7.

2. APPLICATIONS OF D-BAR PROBLEMS AND NUMERICAL APPROACHES

In this section we summarize the main applications of D-bar problems, and review previous numerical approaches for its solution.

2.1. Application 1: The inverse conductivity problem. Briefly, one is given static electric measurements on the boundary of a domain, and the problem is to recover the conductivity in the domain. This is used, for example, in medical Electrical Impedance Tomography. The practical implementation involves tackling several different mathematical problems, one of which is precisely the $\bar{\partial}$ problem which is the topic of this paper. The mathematical formulation centers around the so-called conductivity equation,

$$(9) \quad \nabla \cdot (\gamma(x, y) \nabla u(x, y)) = 0, \quad (x, y) \in \Omega .$$

If one applies a voltage f on the boundary of Ω , one then finds a unique solution to (9) together with the Dirichlet boundary condition

$$(10) \quad u(x, y) = f(x, y), \quad (x, y) \in \partial\Omega .$$

On the other hand, if one knows the current density on the boundary (a function $g(x, y)$), then one can also find a solution to the equation (9) together with the *Neumann* boundary condition

$$(11) \quad \gamma(x, y) \frac{\partial u}{\partial \nu}(x, y) = g(x, y), \quad (x, y) \in \partial\Omega ,$$

where ν is the outward normal to $\partial\Omega$. The business at hand centers on the Dirichlet-to-Neumann mapping, which produces an appropriate Neumann data function g given Dirichlet data f .

The inverse problem, in a nutshell, is to start with the full knowledge of the Dirichlet-to-Neumann mapping, and to determine the conductivity $\gamma(x, y)$ everywhere in Ω . The steps, as outlined in [9], are as follows:

- A. From the Dirichlet-to-Neumann mapping, construct the so-called scattering transform $t(k)$. The steps in constructing this *without direct use of the conductivity equation* are outlined, for example, in [7].
- B. Re-cast the original conductivity equation as a Schrödinger equation in the plane by writing $q = \gamma^{-1/2} \Delta \gamma^{1/2}$, and $\tilde{u} = \gamma^{1/2} u$, so that

$$(12) \quad (-\Delta + q) \tilde{u} = 0, \quad (x, y) \in \Omega ,$$

and then extend q to the entire plane, and seek a solution $\tilde{u} = \psi(x, y, k)$ with the following asymptotics as $|z| \rightarrow \infty$:

$$(13) \quad e^{-ikz} \psi(x, y, k) = 1 + \mathcal{O}\left(\frac{1}{z}\right) .$$

- C. The quantity $\psi(x, y, k)$ solves a D-bar equation *in the variable* k , which is best expressed in terms of $\mu = e^{-ikz} \psi(x, y, k)$:

$$(14) \quad \bar{\partial} \mu = \frac{t(k)}{4\pi k} e^{2i(k_1 x - k_2 y)} \bar{\mu} .$$

- D. The conductivity is extracted from μ by evaluating it at $k = 0$:

$$(15) \quad \lim_{k \rightarrow 0} \mu(x, y, k) = \gamma(x, y)^{1/2} .$$

2.2. Application 2: Integrable nonlinear partial differential equations in 2 + 1 dimensions. The defocusing Davey-Stewartson II equation is the following nonlinear partial differential equation

$$(16) \quad iq_t + \frac{1}{2}(q_{xx} - q_{yy}) = -|q|^2 q + \varphi q$$

$$(17) \quad \varphi_{xx} + \varphi_{yy} = -2(|q|^2)_{xx} .$$

In the above, $q = q(x, y, t) = q(z, t)$ is complex-valued, and subscripts denote partial derivatives. Solutions of this equation can be interpreted (in an idealized sense) as representing the envelope of a two-dimensional surface wave propagating unidirectionally with a specified wave number.

Comment on notation Here and in what follows we will write $\psi(z, k)$ even when ψ is not analytic in z or k .

The Davey-Stewartson II equation (16 - 17) is completely integrable, possessing a Lax-pair

$$(18) \quad \psi_x + i\sigma_3\psi_y = \begin{pmatrix} 0 & q \\ \bar{q} & 0 \end{pmatrix} \psi,$$

$$(19) \quad \psi_t = \begin{pmatrix} i\bar{\partial}^{-1}\partial(|q|^2)/2 & -i\partial q \\ i\bar{\partial}\bar{q} & -i\bar{\partial}^{-1}\partial(|q|^2)/2 \end{pmatrix} \psi - \begin{pmatrix} 0 & q \\ \bar{q} & 0 \end{pmatrix} \psi_y + i\sigma_3\psi_{yy},$$

The equation (18) is referred to, by analogy with previous 1-dimensional cases, as the spectral problem associated to the DS-II equation. It can equivalently be written as

$$(20) \quad \begin{pmatrix} \bar{\partial} & 0 \\ 0 & \partial \end{pmatrix} \psi = \frac{1}{2} \begin{pmatrix} 0 & q \\ \bar{q} & 0 \end{pmatrix} \psi.$$

The *direct problem* is then to seek a vector-valued solution $\psi = \psi(z, k) = \begin{pmatrix} \psi_1 \\ \psi_2 \end{pmatrix}$ with the following asymptotic behavior as $|z| \rightarrow \infty$:

$$(21) \quad \lim_{|z| \rightarrow \infty} \psi_1 e^{-kz} = 1,$$

$$(22) \quad \lim_{|z| \rightarrow \infty} \psi_2 e^{-\bar{k}\bar{z}} = 0.$$

As mentioned above, the quantity ψ is referred to as a CGO solution. The *reflection coefficient*, $r(k)$, is encoded in the sub-leading term in the asymptotic expansion of ψ , via

$$(23) \quad \psi_2 e^{-\bar{k}\bar{z}} = \frac{r(k)}{\bar{z}} + \mathcal{O}\left(\frac{1}{|z|^2}\right).$$

It is customary (though not necessary) to re-cast the equations (20) as a D-bar problem by defining

$$(24) \quad \mu_1 = \psi_1 e^{-kz}, \quad \mu_2 = \bar{\psi}_2 e^{-kz},$$

for then $\mu = \begin{pmatrix} \mu_1 \\ \mu_2 \end{pmatrix}$ solves the D-bar problem

$$(25) \quad \bar{\partial}\mu = \frac{qe^{\bar{k}\bar{z}-kz}}{2} \begin{pmatrix} 0 & 1 \\ 1 & 0 \end{pmatrix} \bar{\mu}.$$

Diagonalizing the above system produces equations of the form (1). Indeed, the matrix $\begin{pmatrix} 0 & 1 \\ 1 & 0 \end{pmatrix}$ has eigenvalues ± 1 , and can be diagonalized via

$$(26) \quad \begin{pmatrix} 0 & 1 \\ 1 & 0 \end{pmatrix} = \begin{pmatrix} 1 & 1 \\ 1 & -1 \end{pmatrix} \sigma_3 \left(\frac{1}{2} \begin{pmatrix} 1 & 1 \\ 1 & -1 \end{pmatrix} \right).$$

If one sets

$$(27) \quad M = \frac{1}{2} \begin{pmatrix} 1 & 1 \\ 1 & -1 \end{pmatrix} \mu,$$

then the entries of $M = \begin{pmatrix} M_1 \\ M_2 \end{pmatrix}$ satisfy

$$(28) \quad \bar{\partial}M_1 = \frac{qe^{\bar{k}\bar{z}-kz}}{2} \bar{M}_1,$$

$$(29) \quad \bar{\partial}M_2 = -\frac{qe^{\bar{k}\bar{z}-kz}}{2} \bar{M}_2,$$

two equations of the form (1), both quantities normalized so that

$$(30) \quad M_j = 1 + \mathcal{O}\left(\frac{1}{z}\right) \text{ as } |z| \rightarrow \infty.$$

. The reflection coefficient is obtained from (28)-(29) via

$$(31) \quad r = \frac{1}{2} \left(M_1^{(1)} - M_2^{(1)} \right)$$

where $M_1^{(1)}$ and $M_2^{(1)}$ represent the $\frac{1}{z}$ coefficients of M_1 and M_2 as $z \rightarrow \infty$:

$$M_1 = 1 + \frac{M_1^{(1)}}{z} + \dots, \quad M_2 = 1 + \frac{M_2^{(1)}}{z} + \dots .$$

As $q = q(x, y, t)$ evolves according to (16-17), the reflection coefficient evolves as well, but the evolution of r is quite simple:

$$(32) \quad r(k, t) = r(k, 0) e^{\frac{-it}{4}(k^2 + \bar{k}^2)} .$$

Better still, the reconstruction of the potential $q(x, y, t)$ given $r(k, 0)$ is achieved via a D-bar problem *in the variable k* , so that in (33-34) below, $\bar{\partial} = \frac{\partial}{\partial \bar{k}}$. Already placing things in diagonal form, the problem is:

$$(33) \quad \bar{\partial} \tilde{M}_1 = e^{\bar{k}\bar{z} - kz} \overline{r(k)} \tilde{M}_1 ,$$

$$(34) \quad \bar{\partial} \tilde{M}_2 = -e^{\bar{k}\bar{z} - kz} \overline{r(k)} \tilde{M}_2 ,$$

together with the normalization conditions

$$(35) \quad \tilde{M}_1 = 1 + \frac{\tilde{M}_1^{(1)}}{k} + \mathcal{O} \left(\frac{1}{|k|^2} \right) \quad \text{as } |k| \rightarrow \infty ,$$

$$(36) \quad \tilde{M}_2 = 1 + \frac{\tilde{M}_2^{(1)}}{k} + \mathcal{O} \left(\frac{1}{|k|^2} \right) \quad \text{as } |k| \rightarrow \infty .$$

The potential $q(x, y, t)$ is then obtained via

$$(37) \quad q(x, y, t) = \tilde{M}_1^{(1)} - \tilde{M}_2^{(1)} .$$

2.3. Application 3: 2D orthogonal polynomials and Normal Matrix Models in Random Matrix Theory. The orthogonal polynomials in this example are denoted $\{p_j = p_j(z)\}_{j=0}^{\infty}$, z is the usual complex variable, and the orthogonality is with respect to the two-dimensional measure $W(x, y)dA$:

$$(38) \quad \iint_{\mathbb{R}^2} \bar{p}_k p_k W(x, y) dA = \delta_{jk} , \quad j, k = 0, \dots .$$

The orthogonality condition is equivalent to the conditions contained in the statement that the following solid Cauchy transform decays rapidly for $z \rightarrow \infty$:

$$(39) \quad \iint \frac{\bar{p}_n(z')}{z' - z} W(x', y') dA' = \mathcal{O} \left(z^{-(n+1)} \right) \quad \text{as } z \rightarrow \infty .$$

Putting this together, one sees that the row vector

$$(40) \quad \bar{\mu} := \left(p_n, \frac{1}{\pi} \iint \frac{\bar{p}_n(z')}{z' - z} W(x', y') dA' \right)$$

solves a d-bar problem: the row vector behaves as follows for $z \rightarrow \infty$:

$$(41) \quad \bar{\mu} \begin{pmatrix} z^{-n} & 0 \\ 0 & z^n \end{pmatrix} = (1, 0) + \mathcal{O} \left(\frac{1}{z^n} \right) ,$$

and $\bar{\mu}$ satisfies

$$(42) \quad \bar{\partial} \bar{\mu} = \bar{\mu} \begin{pmatrix} 0 & -W(x, y) \\ 0 & 0 \end{pmatrix} .$$

For applications to the Normal Matrix Model in Random Matrix Theory, the sort of weight functions that are of interest include those of the form $W = e^{-N(|z|^2 + u(x, y))}$ where the function $u(x, y)$ is a harmonic function whose growth at ∞ is slower than quadratic, so that the integrals are finite. While the analysis of orthogonal polynomials with respect to a weight supported on the real axis (or even, in some cases,

supported on a contour) has been carried out via Riemann-Hilbert techniques, the asymptotic analysis of these polynomials (as the degree grows to ∞ with the parameter N) has defied analysis, except in a select few special examples. On the other hand, their asymptotic behavior is central to a great many applications, from the theory of Normal Random Matrices through to approximation theory.

2.4. Desiderata. For the first two applications described above, what is really required from the D-bar problem is the solution *at a specific point*. In the first example, the conductivity is obtained from the solution to the D-bar problem at $k = 0$, while in the second example, the reflection coefficient is obtained from the coefficient of $\frac{1}{z}$ in the expansion of the solution to the D-bar problem as $|z| \rightarrow \infty$. (The third example, 2D orthogonal polynomials, is more demanding, as the solution is actually required (in applications to the Normal Matrix Model) for all $z \in \mathbb{C}$.)

In all cases, however, reformulating the D-bar equation as an integral equation shows that a starting point is the existence theory for a solution ψ in $L^\infty(\mathbb{C})$, which can then be promoted to a solution with greater regularity if desired.

Thus, in the literature one finds existence theory in L^∞ , for potentials Q in relatively weak spaces, and one of the driving quests has been to obtain existence and uniqueness results under essentially minimal assumptions on the potential Q .

2.5. Brief description of the numerical method developed by Knudsen, Mueller, and Siltanen.

A numerical solution method for (1) was developed and implemented in [18]. The approach taken was to express the fundamental equation (1), normalized so that $\psi = 1 + v$, with $v = \mathcal{O}(1/|z|)$ as $|z| \rightarrow \infty$, in terms of the operator $\bar{\partial}^{-1}$, which is a well-known singular integral operator in \mathbb{C} . The integral equation takes the form

$$(43) \quad v = 1 + \frac{1}{\pi} \iint_{\mathbb{C}} \frac{Q(z')\bar{v}}{z - z'} d^2 z' .$$

(Compare to equation (1.3) in [18], with k replaced by z and $T(k')$ replaced by $Q(z')$.) Because of the application to the inverse conductivity problem, they considered functions Q of compact support. This compact support lent itself to a periodic extension, which they showed restricts to the *actual solution* on the original support. Casting the problem in a periodic setting in turn led them to the use of the fast-Fourier transform in order to evaluate the discretization of the integral operator

$$(44) \quad \mathcal{I}(\varphi) = \int_{-s}^s \int_{-s}^s g(z - z') Q(z') \varphi(z') dz_1 dz_2 ,$$

where $g = g(z)$ represents the periodic extension of the function $\frac{1}{z}$ and the fundamental period domain is $[-s, s]^2$.

In discretizing and periodically extending the function $1/z$, the authors handled the singularity at $z = 0$ by the relatively simple rule

$$(45) \quad g_h(z) = \begin{cases} g(jh), & \text{for } j \in \mathbb{Z}_m^2 \setminus 0, \\ 0, & \text{for } j = 0 . \end{cases}$$

See [18] for a description of the grid, and the finite integer lattice \mathbb{Z}_m^2 .

The authors showed that their method converges as the grid spacing tends to 0, demonstrating that the method is a first order method. The reason the method is first order and does not show spectral convergence of a Fourier approach is this simple regularization: though a Riemann integral does not change if the integrand is just changed in one point, the same is not true for a spectral method, in particular not for a discrete Fourier transform. Changing the function in one point implies that it is not continuous, and it is well known that the Fourier coefficients c_n , $n \in \mathbb{Z}$ for a non-continuous function decrease as $1/n$. Starting from the successful regularization, the authors subsequently developed a two-grid method, based on the work of Vainikko [23]. Note, however, that the authors consider functions of lower regularity than we, and for such functions spectral convergence cannot be observed even with the regularization to be discussed in the following sections. (Moreover, for the intended application to Electrical Impedance Tomography, the available data from measurements is sparse for this ill-posed problem, and so what is required is a lower order, fast approximation scheme.)

Prior to this work, there were other approaches to the numerical solution of the D-bar equation (1). These approaches are described briefly in [18], and we quote from that article, replacing citations with our own citation numbering scheme as needed (equation (1.1) in the quotation below is $\bar{\partial}v(k) = -T(k)v(k)$):

“The numerical solution of equation (1.1) was considered by Siltanen et al [14] for EIT in the numerical algorithm based on Nachman’s uniqueness proof for the 2-D inverse conductivity problem [24]. In [14, 15, 25, 16], equation (1.1) was solved numerically by a 2-D adaptation of the method of product integrals [2]. The numerical solution of equation (1.1) has also been applied to EIT by Knudsen [19] in the numerical algorithm based on the Brown-Uhlmann uniqueness proof for the 2-D inverse conductivity problem [4]. A fast, direct algorithm for the Lippmann-Schwinger equation in two dimensions is found in [5].”

More details can be found in Chapters 14 and 15 of the text book [21]. The basic approach to handling the inverse of the D-bar operator developed in [18] has been used in a number of different applications, see for example [9, 17, 1, 20] and references cited therein. Very recently, in [10], a finite difference solver for the D-bar equation (which was shown to be second order) was implemented to reconstruct EIT images.

3. BRIEF DISCUSSION OF EXISTENCE THEORY FOR EQUATION (1)

In this section we present a brief summary of known existence results for solutions to D-bar problems. As mentioned above, the D-bar equation (1), re-written for the unknown m (3) can be re-cast as a singular integral equation

$$(46) \quad m(x, y) = 1 + \frac{1}{2\pi} \iint_{\mathbb{C}} \frac{Q(z') e^{\overline{kz'} - kz'} \overline{m(z')}}{z - z'} d^2 z' + \frac{1}{2\pi} \iint_{\mathbb{C}} \frac{Q(z') e^{\overline{kz'} - kz'}}{z - z'} d^2 z' ,$$

an integral equation of the form

$$(47) \quad (1 - \mathcal{I}_{Q,k}) m = \mathcal{I}_{Q,k}(1) ,$$

where

$$(48) \quad \mathcal{I}_{Q,k}(f) = \frac{1}{2\pi} \iint_{\mathbb{C}} \frac{Q(z') e^{\overline{kz'} - kz'} \overline{f(z')}}{z - z'} d^2 z' .$$

The existence theory for this equation has been explained in a number of places; we refer to [27] and [26] and references contained therein for the following description of the existence theory. (In those references, the authors were dedicated to establishing global existence for solutions of the Davey-Stewartson II initial value problem. Along the way they had to tackle the existence, uniqueness, and regularity of a coupled version of the above D-bar problem.)

The operator $\mathcal{I}_{Q,k}$ is first shown to be a Fredholm operator of index zero. The goal is to prove that there is nothing in the kernel of the operator $1 - \mathcal{I}_{Q,k}$. If this is successful, Fredholm theory implies that $1 - \mathcal{I}_{Q,k}$ is an invertible operator. A uniform bound on the *inverse* is obtained by first establishing a bound for large k , and then using continuity in k for the bounded subset of the k plane remaining.

This is the original approach taken by Sung [27], who established the existence in $L^\infty(\mathbb{R}^2)$, with potentials in $L^{1,\infty}(\mathbb{R}^2)$ (the space of complex valued bounded and Lebesgue integrable functions on \mathbb{R}^2), and then proceeded to establish differentiability properties of the solution when the potential has derivatives in $L^{1,\infty}(\mathbb{R}^2)$. One particular result of his work (but not the only one) is that the *reflection coefficient* $r(k_1, k_2)$ is in the Schwartz class $\mathbb{S}_{k_1, k_2}(\mathbb{R}^2)$ of functions if the potential $Q(x, y)$ is in $\mathbb{S}_{x,y}(\mathbb{R}^2)$.

Perry [26] iterated the integral equation one time, and thus analyzed integral operators of the form

$$(49) \quad \mathcal{T}(\psi) = \iint_{\mathbb{C}} \frac{e^{\overline{kz'} - kz'} Q}{z - z'} \iint_{\mathbb{C}} \frac{e^{kz'' - \overline{kz''}} \overline{Q}}{z' - z''} \psi(z'') d^2 z'' d^2 z' .$$

He then follows the basic Fredholm theory approach outlined above, assuming now that the potential Q is in $H^{1,1}(\mathbb{R}^2) = \{f \in L^2(\mathbb{R}^2) : \nabla f, (1 + |\cdot|) f(\cdot) \in L^2\}$. Note that we also use a once iterated version of the integral equation (8) in our numerical approach, but there the iteration is done in Fourier space.

Perry proves that if $Q \in H^{1,1}(\mathbb{R}^2)$, then the integral equation he considers (a coupled version of (46)) has a unique solution in $L^\infty(\mathbb{R}^2)$ which in addition is Hölder continuous in z of order α for any $\alpha \in (0, 1)$.

Since the main effort is in establishing that the operator $(1 - \mathcal{I}_{Q,k})$ is invertible, this implies immediately that *our equation* (46) possesses a solution in $L^\infty(\mathbb{R}^2)$ which is also Hölder continuous with exponent α for any $\alpha \in (0, 1)$, and m actually converges to 1 as $|z| \rightarrow \infty$.

Moreover, if we assume that our potential is in $\mathbb{S}_{x,y}(\mathbb{R}^2)$, then once a solution exists which is both bounded and Hölder continuous for $z \in \mathbb{C}$, standard potential theory (see, for example, [6, pp. 53-61]) implies that the right hand side of (46) is Hölder continuous with exponent $\alpha + 1$, which clearly implies that m is infinitely differentiable, and possesses a complete expansion in powers of $\frac{1}{z}$ for $|z| \rightarrow \infty$.

We summarize these facts in a Theorem, which is attributable to the above collection of references:

Theorem 3.1. *Suppose that $Q \in \mathbb{S}_{x,y}(\mathbb{R}^2)$. Then the solution m to the $\bar{\partial}$ equation (4) exists, possesses an expansion in powers of $\frac{1}{z}$ for $z \rightarrow \infty$, which may be differentiated term-by-term to obtain an expansion for derivatives of m . Finally,*

$$(50) \quad \bar{\partial}m \in \mathbb{S}_{x,y}(\mathbb{R}^2) .$$

The last conclusion, (50), follows from the $\bar{\partial}$ equation itself, and is the basis for a spectrally based numerical method. Indeed, it provides rigorous justification for equation (6), re-written here for convenience (recall that $S(\xi) = \xi \hat{m}(\xi)$).

$$(8) \quad S(\xi) = -i\mathcal{F} \left\{ Q e^{\bar{k}z - kz} \left(\overline{\mathcal{F}^{-1} \left(\frac{1}{\xi} S(\xi) \right)} \right) \right\} - i\mathcal{F} \left\{ Q e^{\bar{k}z - kz} \right\} .$$

We close this section with a useful fact.

Lemma 3.2. *Suppose that $h \in \mathbb{S}_{x,y}(\mathbb{R}^2)$. Then*

$$\bar{\partial}^{-1}(h) := \mathcal{F}^{-1} \left(\frac{-2i}{\xi} \mathcal{F}(h) \right)$$

is an infinitely differentiable function, possessing a complete expansion in powers of $\frac{1}{z}$ as $|z| \rightarrow \infty$.

One may see this by writing

$$(51) \quad \mathcal{F}^{-1} \left(\frac{-2i}{\xi} h(\xi_1, \xi_2) \right) = \frac{-i}{\pi} \int_{\mathbb{R}^2} h(r \cos \theta, r \sin \theta) e^{ir(x \cos \theta + y \sin \theta) - i\theta} d\theta dr ,$$

which is clearly infinitely differentiable in x and y . The expansion in powers of $\frac{1}{z}$ follows either from a stationary phase analysis of this integral, or from the alternative representation of $\bar{\partial}^{-1}(h)$:

$$(52) \quad \bar{\partial}^{-1}(h) = \frac{1}{\pi} \iint_{\mathbb{R}^2} \frac{h(x', y')}{z - z'} d^2 z' .$$

4. NUMERICAL ALGORITHM FOR THE SOLUTION OF THE D-BAR PROBLEM

In this section we present an algorithm for the numerical solution of the integral equation (8) for small k . We will take $k = 0$, but the algorithm works for small k as well. The approach follows in principle [18], but uses a more sophisticated regularization of the singular integrand in (8) to provide a sufficiently smooth integrand for the numerical computation of the integral.

4.1. Fourier approach and GMRES. It is a well known fact from Fourier analysis that the Fourier transform of a Schwartz function is itself in a Schwartz space. This is the analytic basis of the efficient implementation of so-called spectral methods, in our case discrete Fourier series, which are used in this paper as follows: the Schwartz functions to be studied are considered on a sufficiently large computational domain,

$$(53) \quad x \in L_x[-\pi, \pi], \quad y \in L_y[-\pi, \pi],$$

that the function and its derivatives decrease to machine precision (here roughly 10^{-16} , but in practice limited due to rounding errors to 10^{-14} or less) at the boundaries. This allows to treat Schwartz functions as smooth periodic functions within machine precision. In this case the Fourier coefficients decrease also

exponentially. Approximating the Fourier series with a discrete Fourier series (computed efficiently via an FFT), which corresponds in a sense to a truncation, the numerical error by neglecting the Fourier coefficients c_n with $n > N/2$ will decrease exponentially with N , i.e., faster than any power of $1/N$. A method being in this sense of infinite order is called a spectral method. We always choose the wave numbers in the FFT as

$$(54) \quad \xi_1 \in [-N_x/2 + 1, N_x/2]/L_x, \quad \xi_2 \in [-N_y/2 + 1, N_y/2]/L_y,$$

where N_x and N_y are the number of Fourier modes in the x and y direction respectively. The values of N_x and N_y are chosen in a way that the Fourier transform of the studied Schwartz function decreases to machine precision as ξ_1 and ξ_2 approach the boundary of the computational domain.

The discrete Fourier approach implies that the integral equation (8) is approximated by a finite dimensional system of linear equations. Writing the $N_x \times N_y$ matrix S as a vector with $N_x N_y$ components, this system of equations has the form $\mathcal{A}S = b$. As in [18], we use GMRES [22] Krylov subspace techniques to solve this linear system. The advantage of GMRES is that the $N_x N_y \times N_x N_y$ matrix \mathcal{A} does not have to be stored (this would make the use of parallel computers necessary for some of the values of N_x, N_y used here), just its action on a vector has to be known. The price to pay for this memory efficient implementation is that the equation $\mathcal{A}S = b$ is solved iteratively with a certain tolerance that can be chosen. For the high precision experiments to be presented below, we typically use a tolerance of the order of machine precision (in practical application, this can be of course chosen larger). In practice GMRES converges rapidly in the studied examples.

4.2. Regularization of the integrand. To obtain spectral convergence the goal is to provide smooth periodic functions for all numerical evaluations involving an FFT. Obviously this is not the case for the function $S(\xi)/\xi$ in (8), which is not even bounded for $\xi \rightarrow 0$, though $S(\xi)$ is a smooth function, as explained in Theorem 3.1. To address the problem of $S(\xi)/\xi$ not being in the Schwartz class, the idea is to write the related integral in the form

$$(55) \quad \mathcal{F}^{-1} \left(\frac{1}{\xi} S(\xi) \right) = \mathcal{F}^{-1} \left(\frac{1}{\xi} (S(\xi) - G(\xi)) \right) + \mathcal{F}^{-1} \left(\frac{1}{\xi} G(\xi) \right),$$

where $G(\xi)$ is chosen in a way that $(S(\xi) - G(\xi))/\xi$ is (within numerical precision) a smooth rapidly decreasing function, and that $\mathcal{F}^{-1}(G(\xi)/\xi)$ can be given in explicit form analytically up to constants which can also be computed with spectral accuracy. If this is possible, spectral convergence can be expected since $\mathcal{F}^{-1}(G(\xi)/\xi)$ will be multiplied with a Schwartz function, and thus the Fourier transform on the right hand side of (55) can be computed with the wanted precision.

To identify a suitable function $G(\xi)$ in (55), we use the following

Lemma 4.1. *The inverse Fourier transform of $\exp(-|\xi|^2)/\xi$ is given by*

$$(56) \quad \mathcal{F}^{-1} \left(\frac{1}{\xi} e^{-|\xi|^2} \right) = \frac{i}{x + iy} \left(1 - e^{-(x^2 + y^2)/4} \right).$$

In addition one has

$$(57) \quad \mathcal{F}^{-1} \left(\frac{\bar{\xi}^n}{\xi} e^{-|\xi|^2} \right) = i(2i)^n \frac{n!}{z^{n+1}} \left\{ 1 - \exp \left(-\frac{|z|^2}{4} \right) \sum_{k=0}^n \frac{1}{k!} \left(\frac{z\bar{z}}{4} \right)^k \right\},$$

which is equivalent to

$$(58) \quad \mathcal{F}^{-1} \left(\frac{\bar{\xi}^n}{\xi} e^{-|\xi|^2} \right) = i(2i)^n n! \left(\frac{\bar{z}}{4} \right)^{n+1} \sum_{k=0}^{\infty} \frac{1}{(k+n+1)!} \left(\frac{z\bar{z}}{4} \right)^k.$$

Relation (56) can be established by direct calculation, whereas the remaining equations follow from it via

$$(59) \quad \mathcal{F}^{-1} \left(\frac{\bar{\xi}^n}{\xi} e^{-|\xi|^2} \right) = (-2i\partial_z)^n \frac{i}{z} \left(1 - \exp(-|z|^2/4) \right),$$

by direct calculation.

Remark 4.2. The term in (58) is similar to so-called ϕ -functions appearing in ETD schemes, see for instance [11] and references therein. This formula is numerically problematic close to the origin (say for $|z| < 1$), because of cancellation errors. There it is more convenient to use the Taylor expansion (58). This allows one to compute the function to machine precision in the whole computational domain.

Remark 4.3. Lemma (4.1) permits the construction of a function $G(\xi)$ in (55) such that $(S(\xi) - G(\xi))/\xi$ is a Schwartz function. A possible choice is $G(\xi) = S(\xi) \exp(-|\xi|^2)$, which implies, however, that the last integral on the right hand side of (55) can only be computed as a convolution,

$$(60) \quad \mathcal{F}^{-1} \left\{ S e^{-|\xi|^2} / \xi \right\} = \frac{1}{2\pi} \int \mathcal{F}^{-1}(S) \frac{i}{z - z'} \left(1 - e^{-\overline{(z-z')}(z-z')/4} \right) d^2 z' .$$

This choice of $G(\xi)$ satisfies all requirements, but the computation of the convolution is not very efficient since the standard Fourier approach would involve functions of lower regularity than wanted (exactly the function $\exp(-|\xi|^2)/\xi$ introduced since it has an analytically known Fourier transform). Thus to obtain a spectral method, the convolution has to be computed directly, which is computationally expensive, since the integrand is an object in four real dimensions. It will be shown in this and the following section how a two-dimensional approach can be realized. Nonetheless we use a code implementing this approach to provide an independent test of other codes.

The nature of the singularity of $S(\xi)/\xi$ at $\xi = 0$ is demonstrated by a two-dimensional Taylor expansion:

$$\frac{1}{\xi} S(\xi) = \frac{S(0,0)}{\xi} + \sum_{j=1}^M \frac{1}{j!} \frac{\partial^j}{\partial \bar{x}^j} S(0,0) \left(\frac{\bar{\xi}^j}{\xi} \right) + \text{regular} .$$

The term “regular” possesses M continuous derivatives, and the first two terms clearly possess only fewer derivatives at $\xi = 0$. Closer inspection shows that the first two terms can be thought of as the purely anti-holomorphic part of S , divided by ξ . Thus we choose G so as to eliminate these terms:

$$(61) \quad G(\xi) = e^{-|\xi|^2} \sum_{n=0}^M \frac{1}{n!} \frac{\partial^n S(0)}{\partial \bar{\xi}^n} \bar{\xi}^n ,$$

where M is taken large enough that the Fourier coefficients of $(S(\xi) - G(\xi))/\xi$ decrease to machine precision. (To see this, observe that $(S(\xi) - G(\xi))/\xi$ possesses M continuous derivatives, and decays rapidly to zero for $|\xi|$ approaching the boundary of the computational domain, and hence its Fourier coefficients will decrease rapidly as well). The derivatives of S in (61) are numerically computed via

$$(62) \quad \frac{\partial^n S(0)}{\partial \bar{\xi}^n} = \left(-\frac{i}{2} \right)^n \mathcal{F} z^n \mathcal{F}^{-1} S ,$$

i.e., also with FFT techniques which can be done with spectral accuracy since S is a Schwartz function. Note, however, that for large n , the multiplication with z^n in (62) will delimit the achievable numerical accuracy.

To test the above approach to compute the inverse of the D-bar derivative for Schwartz functions via Fourier integrals, we consider the following test problem: It is straightforward to show by direct calculation that

$$(63) \quad \partial_{\bar{z}}^{-1} \exp(-a(z-b)(\bar{z}-c)) = \frac{a}{z-b} (1 - \exp(-a(z-b)(\bar{z}-c))) ,$$

where $a > 0$, b, c are constants. In Fig. 1 we show how the difference between the numerical and the exact solution depends on the number of Fourier modes and the number M of terms in the Taylor expansion of S in (61). For simplicity we use $N_x = N_y = N$ Fourier modes and $L_x = L_y = 4$.

The left figure shows the dependence of the L^∞ norm of the difference between numerical and exact solution on the number M of terms in the Taylor series in (61), using $N = 128$ Fourier modes in both x and y directions. It can be seen in the logarithmic plot that the numerical error decreases exponentially to machine precision. It saturates in this example roughly for $M = 11$. This behavior can be understood as follows: as explained above, the function $(S(\xi) - G(\xi))/\xi$ possesses M continuous derivatives and decreases rapidly to machine precision as ξ approaches the boundary of the computational domain. It is well known

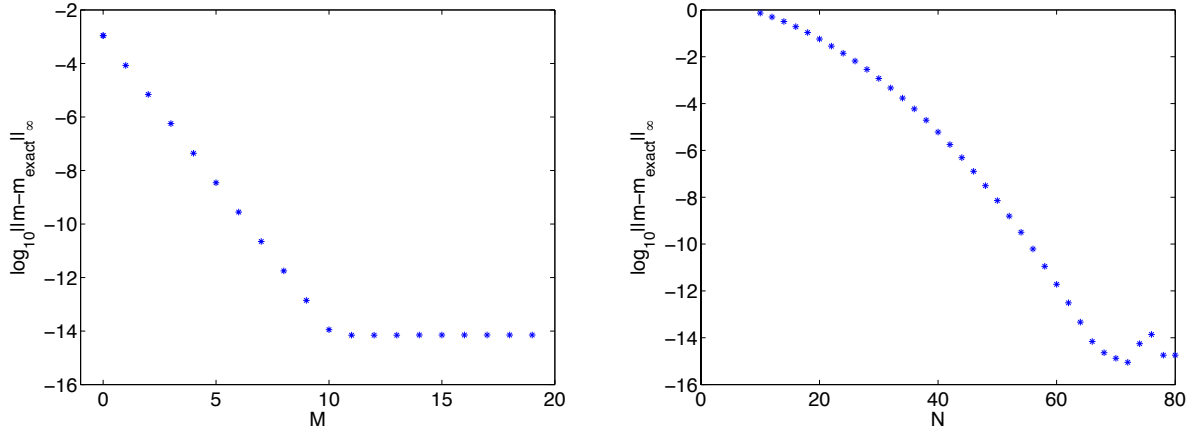


FIGURE 1. Difference between the numerical solution of the D-bar inversion (63) with $a = 1/2$, $b = 1$ and $c = i$. On the left we plot the dependence on the number M of terms in the Taylor expansion (61), with $N = 128$ Fourier modes in x and y . On the right we plot the dependence on the number of Fourier modes N in x and y , using $M = 11$ terms in the Taylor expansion.

that the Fourier coefficients of such a function decrease algebraically in the number N of Fourier modes as $N^{-(M+2)}$. This implies a numerical error of the same order if the series is approximated by a truncated series, and thus we should, and do, see an exponential decrease of the error with M . Note that due to the finite precision of the numerics, it does not make sense to take arbitrarily high values of M . As mentioned above, numerical precision is lost for large values of M in the computation of the derivatives (62) since the integrand is multiplied with high powers of z in (62) and $\bar{\xi}$ in (61). Still it is possible to use values of M up to 20 since with larger M also the functions W_n become smaller at the boundaries, and $\exp(-|\xi|^2)$ is small there in any case.

In a similar way we study in the right figure of Fig. 1 the dependence of the numerical error on the number of Fourier modes N for fixed $M = 11$ (the result does not change if a higher value of M is taken). It can be seen that the numerical error also decreases essentially exponentially and reaches machine precision for $N \approx 2^6$.

4.3. Algorithm for computing a solution to the D-bar equation (8). We present a brief summary for the algorithm to solve (8), with $k = 0$.

- (1) Introduce a discrete Fourier grid as in (53) and (54).
- (2) Compute and store the functions

$$(64) \quad \frac{1}{n!} W_n = \frac{1}{n!} \mathcal{F}^{-1} \left(\frac{\bar{\xi}^n}{\xi} e^{-|\xi|^2} \right)$$

using definitions (57) and (58).

- (3) Call GMRES with $b = -i\mathcal{F}Q$ and $\mathcal{A}S = S + i\mathcal{F} \left(Q \overline{\mathcal{F}^{-1}(S/\xi)} \right)$.
- (4) To compute $\mathcal{A}(S)$:
 - (a) Compute the relevant Taylor coefficients of S at $\xi = 0$, using FFT techniques:

$$n!c_n = \frac{\partial^n}{\partial \bar{\xi}^n} S(0) = \left(\frac{-i}{2} \right)^n \mathcal{F} \left(z^n \mathcal{F}^{-1}(S) \right) (0) .$$

(b) Form

$$(65) \quad \begin{aligned} G(\xi) &= e^{-|\xi|^2} \sum_{n=0}^M c_n \bar{\xi}^n, \\ \mathcal{F}^{-1} \left(\frac{1}{\xi} G(\xi) \right) &= \sum_{n=0}^M c_n W_n. \end{aligned}$$

(c) Now compute the intermediate quantity:

$$(66) \quad h = \mathcal{F}^{-1} \left(\frac{S(\xi)}{\xi} \right) = \mathcal{F}^{-1} \left[\frac{1}{\xi} (S(\xi) - G(\xi)) \right] + \sum_{n=0}^M c_n W_n.$$

(d) And finally compute $\mathcal{A}(S)$:

$$\mathcal{A}(S) = S + i\mathcal{F}(Q \bar{h}).$$

Note that no factorials $n!$ that could affect the accuracy need to be computed here, since they cancel in the combination $W_n c_n$. Factorials just appear in the Taylor series (58).

Remark 4.4. The computational cost of the algorithm is mainly in the FFT commands (always in two dimensions) in the GMRES iterations. The functions W_n in (64) are computed and stored beforehand since they do not change during the iteration. The action of the matrix \mathcal{A} in each GMRES iteration requires two FFTs. In addition the computation of the Taylor coefficients of S in (66) requires one additional FFT (not two, since the values are just needed for $\xi = 0$, the second Fourier transform in (62) can be replaced by a summation). To sum up, per GMRES iteration 3 FFTs are necessary. Thus the computational cost is higher than in [18] (one FFT more per iteration), but the convergence of our approach is spectral instead of first order. When dealing with potentials of sufficient regularity (as we do), we may reach much higher precision with less resolution.

5. NUMERICAL COMPUTATION OF COMPLEX GEOMETRICAL OPTICS SOLUTIONS

In this section we will present a numerical approach to efficiently solve the D-bar equation (4) for general $k \in \mathbb{C}$ with FFT methods. Since the equation (8) defined on \mathbb{R}^2 is approximated by a finite dimensional system on \mathbb{T}^2 , the quality of the approximation will depend on the commensurability of the functions under consideration with the computational domain. The presence of the term $e^{(\bar{k}z - kz)}$ in (8) implies a shift in Fourier space. So, for example, $\mathcal{F}(e^{(\bar{k}z - kz)} Q)$ will not vanish with numerical precision on the boundary of the computational Fourier domain for $|k|$ sufficiently large. Since this was the basis of the approach detailed in the previous section, a reformulation of (8) is necessary in order to apply the same techniques as before.

5.1. Dependence on the parameter k . It is useful to re-express the fundamental equation (8) using an integral operator:

$$(67) \quad S = \mathcal{K}(S) - i\mathcal{F} \left(Q e^{\bar{k}z - kz} \right),$$

where

$$(68) \quad \mathcal{K}(h) = -i\mathcal{F} \left(q e^{\bar{k}z - kz} \left[\mathcal{F}^{-1} \left(\frac{h}{\xi} \right) \right] \right).$$

The operator \mathcal{K} is the composition of a simpler integral operator and a shift:

$$(69) \quad \begin{aligned} \mathcal{K}(h) &= \mathcal{K}_0(h) \circ (\xi + 2i\bar{k}), \\ \mathcal{K}_0 &= -i\mathcal{F} \left(q \left[\mathcal{F}^{-1} \left(\frac{S}{\xi} \right) \right] \right). \end{aligned}$$

For sufficiently small values of k , the numerical approach described in the previous section provides a spectrally accurate discretization of the equation, and the operator acting on S_{\pm} can be directly inverted via GMRES [22].

For larger values of $|k|$, this procedure encounters a new difficulty. Asymptotic analysis of the integral operator \mathcal{K} for $|k|$ large shows that it is a small norm operator, and we may invert the equation by Neumann series for $|k|$ sufficiently large. The first term of this expansion is obviously the last term on the right hand side of (67):

$$(70) \quad S(\xi) \approx S^{(0)} = -i\mathcal{F} \left\{ Q e^{\overline{kz} - kz} \right\} = -i\hat{Q}(\xi + 2i\bar{k}) .$$

Further iterations may be carried out, and so, for example, a more accurate approximation to the solution is obtained by substituting $S^{(0)}$ into the right hand side of equation (67):

$$(71) \quad S(\xi) \approx -i\mathcal{F} \left\{ Q e^{\overline{kz} - kz} \left(\overline{\mathcal{F}^{-1} \left(\frac{1}{\xi} \left(-i\hat{Q}(\xi + 2i\bar{k}) \right) \right)} \right) \right\} - i\hat{Q}(\xi + 2i\bar{k}) .$$

This may be simplified to the following form:

$$(72) \quad S \approx S^{(0)} + S^{(1)},$$

where

$$(73) \quad S^{(1)} = -i\mathcal{F} \left[\frac{q}{2(\bar{z} - \bar{k})} \left[e^{\overline{kz} - kz - |k|^2/4} - e^{-|z|^2} \right] \right] .$$

The above asymptotic description provides a key insight into the numerical issues we are facing for k large. The last term is a shift of \hat{Q} , and is supported in a neighborhood of $-2i\bar{k}$, which can be very near the boundary of the computational domain. Moreover, the *first term* on the right hand side is itself the sum of two terms, the first also being supported in a neighborhood of $-2i\bar{k}$ (although exponentially suppressed by the term $e^{-|k|^2/4}$), and the second term supported near $\xi = 0$. So the solution has support in two disparate regimes, one near the boundary of the computational domain and the other in the middle. This behavior can be seen for instance in Fig. 2.

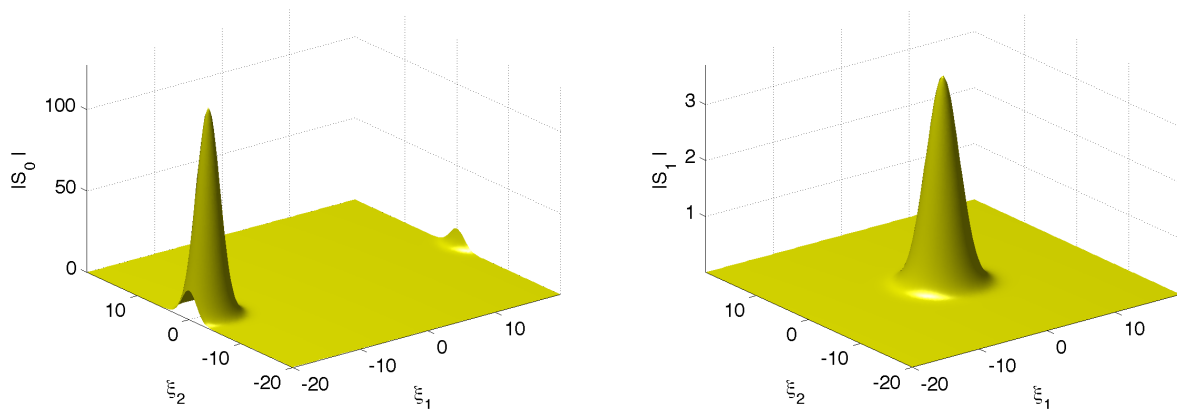


FIGURE 2. Modulus of the iterates S_0 (70) and S_1 (73) for $k = 8.5936$, $L = 3.2$ and $N = 128$.

In the original numerical approach, we are dividing by ξ , which is not periodic, and not very small at the boundary of the computational domain. This has the effect of introducing a discontinuity across the boundary of the computational domain, an anathema to spectral methods.

However, if we know beforehand that a function f has the property that its Fourier transform \hat{f} has support centered at $-i\bar{k}$, we may compute $\bar{\partial}^{-1}(f)$ by exploiting the shift to our advantage:

$$(74) \quad \bar{\partial}^{-1}(f) = -2i\mathcal{F}^{-1} \left[\frac{\hat{f}}{\xi} \right] = -2i\mathcal{F}^{-1} \left[\left(\frac{\hat{f}(\xi - 2i\bar{k})}{\xi - 2i\bar{k}} \right) \circ (\xi + 2i\bar{k}) \right]$$

$$(75) \quad = -2ie^{\bar{k}z - kz} \mathcal{F}^{-1} \left[\left(\frac{\hat{f}(\xi - 2i\bar{k})}{\xi - 2i\bar{k}} \right) \right].$$

Now in this last formula, the numerator, $\hat{f}(\xi - 2i\bar{k})$ is supported, by assumption, in a vicinity of $\xi = 0$, and decays rapidly as $|\xi|$ approaches the boundary of the computational domain. We may then apply the regularization approach of the previous section, but with the singularity at $\xi = 2i\bar{k}$ instead of $\xi = 0$. Precisely, we take

$$(76) \quad G(\xi) = e^{-|\xi - 2i\bar{k}|^2} \sum_{n=0}^M \frac{1}{n!} \frac{\partial^n}{\partial \bar{\xi}^n} \hat{f}(0, 0) (\bar{\xi} + 2i\bar{k})^n,$$

and then

$$(77) \quad \bar{\partial}^{-1}(f) = -2ie^{\bar{k}z - kz} \mathcal{F}^{-1} \left[\left(\frac{\hat{f}(\xi - 2i\bar{k}) - G(\xi)}{\xi - 2i\bar{k}} \right) \right] - 2ie^{\bar{k}z - kz} \mathcal{F}^{-1} \left[\left(\frac{G(\xi)}{\xi - 2i\bar{k}} \right) \right].$$

We demonstrate the effectiveness of this shifting argument in Fig. 3 where we compute the solution to the example (63) for parameters leading to support of the function near the computational boundary with the approach of the previous section, both with and without the shifting argument (77). It can be seen that the numerical solution converges as expected very slowly to the exact one without a shift since the integrand is not small on the boundary. A shift of the integrand in Fourier space such that its maximum is localized near the center of the computational domain restores rapid convergence as in the previous section.

However, it is important to recall that the CGO solutions which we seek are actually supported (for large k) in two disparate regions.

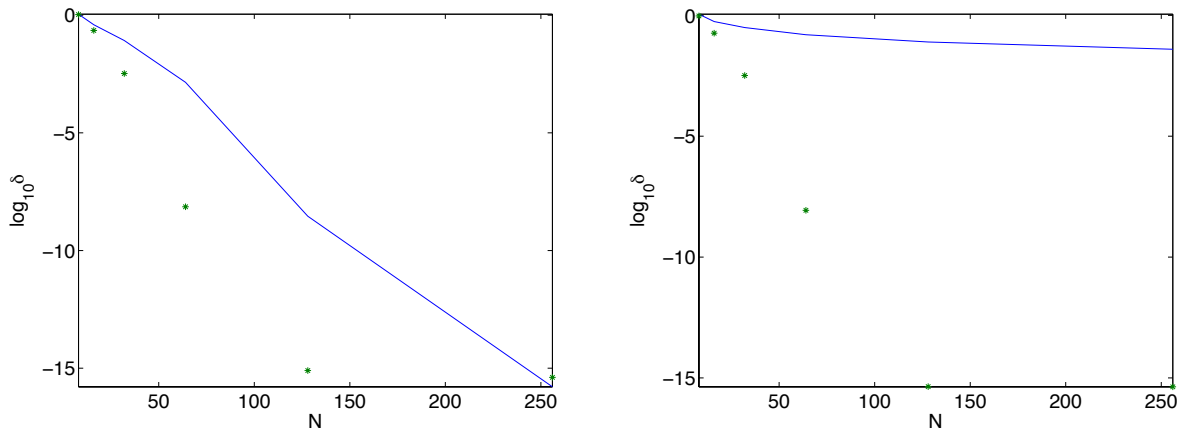


FIGURE 3. These are logarithmic plots of the dependence of the error in computing (63) on N , the number of Fourier modes. The solid line shows the result of the computation without a shift in Fourier space, and the stars show the results with shifting. On the left, the parameters in (63) were chosen so that the Fourier transform of (63) is supported midway between the origin and the boundary of the computational domain. On the right the parameters were chosen so that the Fourier transform of (63) is supported very near the boundary of the computational domain. For these plots, the choice of k varies with N , and the relevant parameter values are summarized in the Table shown in Fig. 4.

Fourier Modes	L	Left Figure k	Right Figure k
2^3	4.0	$0.25(1 + 2i)$	$0.5(1 + i)$
2^4	4.0	$0.5(1 + 2i)$	$1 + i$
2^5	4.0	$(1 + 2i)$	$2(1 + i)$
2^6	4.0	$2(1 + 2i)$	$4(1 + i)$
2^7	4.0	$4(1 + 2i)$	$8(1 + i)$
2^8	4.0	$8(1 + 2i)$	$16(1 + i)$

FIGURE 4. Parameter values for the plots shown in Fig. 3.

5.2. Iterated integral equation. To capture the “disparate regions of support” suggested by the asymptotic analysis, we seek a solution S of the form

$$(78) \quad S = f(\xi) + h \circ (\xi + 2i\bar{k}) ,$$

where h and f are functions supposed to vanish on the computational boundary and to have support in the vicinity of the origin. This leads to a pair of equations:

$$(79) \quad h = \mathcal{K}_0(f) - i\mathcal{F}(q) .$$

$$(80) \quad f = \mathcal{K}_0(h \circ (\xi + 2i\bar{k})) \circ (\xi + 2i\bar{k}) ,$$

Replacing f_{\pm} in the first equation above, we have

$$(81) \quad h - \mathcal{K}_0(\mathcal{K}_0(h \circ (\xi + 2i\bar{k})) \circ (\xi + 2i\bar{k})) = -i\mathcal{F}(q) .$$

Note that this equation is equivalent to Perry’s integral equation (49), but that we consider it in Fourier space. Then we find

$$(82) \quad f = \mathcal{K}_0(h \circ (\xi + 2i\bar{k})) \circ (\xi + 2i\bar{k}) .$$

It will turn out that in the application to the Davey Stewartson II equation, the function f is not needed, it just appears in the above derivation, but all the relevant information about the reflection coefficient is contained in the function h .

It is useful to simplify the integral equation (81) by first noting that

$$(83) \quad \mathcal{K}_0(h \circ (\xi + 2i\bar{k})) \circ (\xi + 2i\bar{k}) = -i\mathcal{F}\left(q \left[\overline{\mathcal{F}^{-1}\left(\frac{h}{\xi - 2i\bar{k}}\right)} \right]\right) ,$$

so that the integral equation (81) becomes

$$(84) \quad h - \mathcal{K}_0\left(-i\mathcal{F}\left(q \left[\overline{\mathcal{F}^{-1}\left(\frac{h}{\xi - 2i\bar{k}}\right)} \right]\right)\right) = -i\mathcal{F}(q) .$$

The above simplification follows from a straightforward calculation:

$$(85) \quad \mathcal{K}_0(h \circ (\xi + 2i\bar{k})) \circ (\xi + 2i\bar{k}) = -i\mathcal{F}\left(q \left[\overline{\mathcal{F}^{-1}\left(\frac{h \circ (\xi + 2i\bar{k})}{\xi}\right)} \right]\right) \circ (\xi + 2i\bar{k})$$

$$(86) \quad = -i\mathcal{F}\left(q \left[\overline{\mathcal{F}^{-1}\left(\frac{h}{\xi - 2i\bar{k}}\right) \circ (\xi + 2i\bar{k})}\right]\right) \circ (\xi + 2i\bar{k})$$

$$(87) \quad = -i\mathcal{F}\left(q \left[\overline{e^{kz - \bar{k}z} \mathcal{F}^{-1}\left(\frac{h}{\xi - 2i\bar{k}}\right)}\right]\right) \circ (\xi + 2i\bar{k})$$

$$(88) \quad = -i\mathcal{F}\left(q \left[\overline{\mathcal{F}^{-1}\left(\frac{h}{\xi - 2i\bar{k}}\right)}\right]\right)$$

5.3. Algorithm to compute CGO solutions. As in section 4, we introduce a standard discretisation of x, y and the dual Fourier variables ξ_1, ξ_2 . The role of the variable k is in a sense also dual to z as can be seen from equation (8). Thus we choose $2k$ on the same grid as ξ . The algorithm to compute the CGO solutions via (84) is thus as follows:

- For given k , approximate (84) as in section 4 by discretizing z and ξ .
- Solve the resulting linear system for the resulting vector h with GMRES.
- The task of computing the left hand side of (84) breaks into two parts:
 - (1) Compute $\mathcal{F}^{-1}\left(\frac{h}{\xi-2i\bar{k}}\right)$ by the shifting and regularization argument explained in (77), and then compute

$$(89) \quad H := -i\mathcal{F}\left(q\left[\overline{\mathcal{F}^{-1}\left(\frac{h}{\xi-2i\bar{k}}\right)}\right]\right).$$

- (2) Finally, compute $\mathcal{K}_0(H)$ by using the previous regularization argument from Section 4.

The computational cost is roughly twice the one of the algorithm of section 4 since the latter algorithm has to be applied twice (mainly 6 two-dimensional FFT per iteration). The advantage is that machine precision can be reached with much smaller values of N_x, N_y for all values of k with the present algorithm.

6. TIME DEPENDENCE OF DS II SOLUTIONS

In this section we study the time dependence of DS II solutions $q(x, y, t)$ for given initial data $q(x, y, 0)$.

Parameter Convention: As noted in Subsection 5.3, it is convenient to choose $2k$ on the same grid as ξ . In this Section, we make that choice, by replacing k with $k/2$, so that k and ξ are dual variables and live on the same grid.

6.1. Construction of solutions to the DS II equation via D-bar problems. Recall that the D-bar equation associated to the DS II equation is the system (28)-(29), normalized by (29). Writing S_+ for $\xi\hat{M}_1$, and S_- for $\xi\hat{M}_2$, we have two equations:

$$(90) \quad S_{\pm}(\xi) = \mp i\mathcal{F}\left\{Qe^{\frac{\bar{k}z-kz}{2}}\left(\overline{\mathcal{F}^{-1}\left(\frac{1}{\xi}S_{\pm}(\xi)\right)}\right)\right\} \mp i\mathcal{F}\left\{Qe^{\frac{\bar{k}z-kz}{2}}\right\}.$$

For each equation, we seek to represent the solution in the form (78):

$$S_{\pm} = f_{\pm}(\xi) + h_{\pm} \circ (\xi + i\bar{k}).$$

It is straightforward to verify, following the same calculations from (78) to (81), that

$$(91) \quad h_{\pm} = \pm h,$$

where h solves the equation

$$(92) \quad h - \mathcal{K}_0(\mathcal{K}_0(h \circ (\xi + i\bar{k})) \circ (\xi + i\bar{k})) = -i\mathcal{F}(q).$$

Moreover,

$$f_+ = f_- = \mathcal{K}_0(h \circ (\xi + i\bar{k})) \circ (\xi + i\bar{k}).$$

For a given value of $k \in \mathbb{C}$, the reflection coefficient is obtained from the computed function h via

$$(93) \quad r(k) = ih(i\bar{k}).$$

This can be seen by first writing a basic representation formula for m_{\pm} :

$$(94) \quad m_{\pm} = \frac{1}{\pi} \iint_{\mathbb{C}} \frac{\bar{\partial} m_{\pm}}{z - z'} d^2 z',$$

from which one may read off the $\mathcal{O}\left(\frac{1}{z}\right)$ term in the large z expansion:

$$(95) \quad m_{\pm}^{(1)} = \frac{1}{\pi} \iint_{\mathbb{C}} \bar{\partial} m_{\pm} d^2 z' = (i\xi \hat{m}_{\pm})|_{\xi=0} = iS_{\pm}(0).$$

Now formula (93) for the reflection coefficient follows from (95) along with (78), (91), and (82).

To solve the DS II equation then, we compute as described above the reflection coefficient (93) and obtain its time dependence from (32). It can be seen that the latter has a rather simple form which immediately implies that $|r|$ is constant in time which is equivalent to the existence of an infinite number of conserved quantities reflecting the complete integrability of the DS II equation. The most prominent conserved quantities are the L^2 norm of q and the energy

$$(96) \quad E = \iint_{\mathbb{R}^2} \left[|\partial_x q(x, y, t)|^2 - |\partial_y q(x, y, t)|^2 + |q(x, y, t)|^4 - \frac{1}{2} (\phi(x, y, t)^2 + (\partial_x^{-1} \partial_y \phi(x, y, t))^2) \right].$$

It is well known that conserved quantities, the conservation of which is not implemented in the code, provide a test for numerical schemes. In [13] it was shown that the error in the numerical conservation of the DS II energy tends to overestimate the numerical accuracy of the solution in an L^∞ sense by two to three orders of magnitude.

It is a remarkable fact of integrable systems that the inverse scattering techniques, here a D-bar problem, immediately allow to go to the final time t one is interested in. The standard approach is as follows: determine the reflection coefficient $r(k, 0)$ as discussed in the previous section by solving (81) for given $q(x, y, 0)$. Then solve the same equation with $r(k, t)$ via (32) after interchanging q and r , and z and k . Thus in contrast to the direct numerical solution of DS II as in [13], no intermediate time steps have to be computed. One just needs to solve twice integral equations of the form (81) for all considered values of k and z .

6.2. Reconstruction of the initial data at $t = 0$. A first test of this approach is to recover the potential $q(x, y, 0)$ from the reflection coefficient $r(k, 0)$. To this end one fixes the parameters L_x, L_y in (53) and N_x, N_y in (54). Maximal precision can only be reached for if both $q(x, y, 0)$ and its Fourier transform decrease to machine precision at the boundaries of the considered domains. Thus if one wants to study the dependence of the difference between the computed $q(x, y, 0)$ via the reflection coefficient and the original $q(x, y, 0)$ on the parameters $L_x = L_y = L$ and $N_x = N_y = N$, the pairs L, N have to be chosen such that both $q(x, y, 0)$ and its Fourier transform decrease roughly to the same order of magnitude. If this is respected, then the numerical error decreases as expected exponentially, see the table in Fig. 5. It shows that the initial data can be recovered to better than 10^{-13} with $N = 256$ Fourier modes in each direction.

Fourier Modes	L	Error
2^3	0.7515	7.09e-03
2^4	1.075	3.1872e-04
2^5	1.5	1.665e-06
2^6	2.1213	1.736e-09
2^7	3.2	2.40e-13
2^8	4.2	5.0e-14

FIGURE 5. Values of number N of Fourier modes and L for $M = 11$ such that both the reconstructed potential $q(x, y, 0)$ and the reflection coefficient decrease to roughly the same precision at the boundaries of the respective computational domains, and the corresponding errors in the reconstruction of the initial data $q(x, y, 0) = \exp(-x^2 - y^2)$ after solving twice equations of the form (81).

6.3. DS II solutions for $t > 0$. It is known from the linear Schrödinger equation that Gaussian initial data are dispersed with time. A similar effect is to be expected in the case of the DS II solution. Thus parameters optimized for $t = 0$ will in general not provide the same resolution for $t > 0$. The reason is that in addition to the dispersive effects of DS II, there will be increasingly oscillations in the real and imaginary part of the DS II solution, see Fig. 6. Nonetheless, when we consider the final time $t = 0.8$, the computed solution still conserves the energy to an error of order 10^{-14} . Of course, larger values of t will require higher resolutions, which does not pose a principle obstacle, but might be best done on parallel computers, see the comments in the following section.

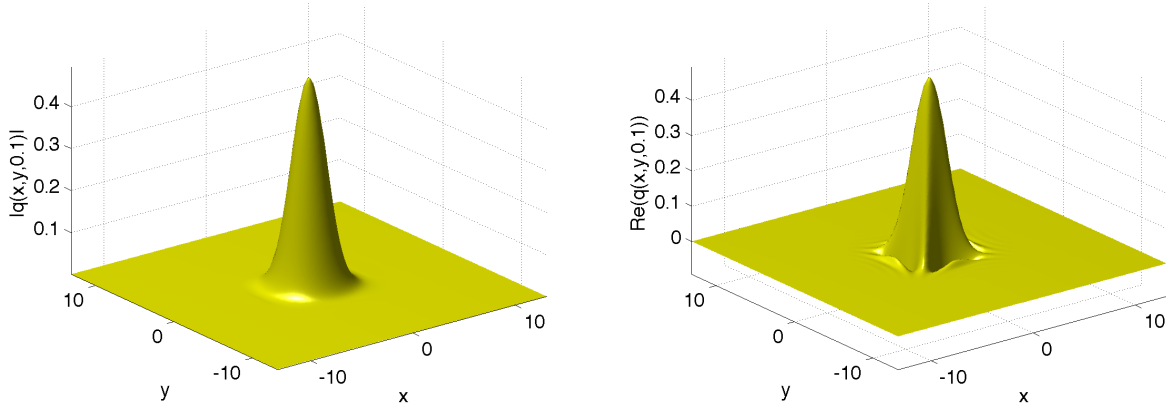


FIGURE 6. Solution to the DS II equation for the initial data $q(x, y, 0) = \exp(-x^2 - y^2)$ for $t = 0.8$; on the left the modulus of the solution, on the right the real part.

The D-bar code can be used as a benchmark for direct solvers. For initial data in $\mathcal{S}(\mathbb{R}^2)$, FFT techniques are again the appropriate method for such solvers. The DS II equation (16) and (17) can be written in Fourier space in the form

$$(97) \quad i(\mathcal{F}q)_t - (\xi_1^2 - \xi_2^2)\mathcal{F}q - \mathcal{F} \left[\mathcal{F}^{-1} \left(\frac{\xi_1^2 - \xi_2^2}{\xi_1^2 + \xi_2^2} \mathcal{F}(|q|^2) \right) q \right] = 0;$$

here equation (17) has been solved in Fourier space to eliminate the function φ in (16). Approximating the Fourier transform as in the previous sections via a discrete Fourier transform, one ends up for (97) with a finite dimensional system of ODEs in t which are then numerically integrated with respect to t . The first approach along these lines appears to have been realised in [28]. More recently, in [13], fourth order stiff integrators for DS II have been studied.

The inversion of the Laplace operator in (17) has introduced the term $(\xi_1^2 - \xi_2^2)/(\xi_1^2 + \xi_2^2)$ in (97). This term is much better behaved than the term $1/(\xi_1 + i\xi_2)$ appearing in the solution of the D-bar problem, but it is still a problem for a spectral approach. This can be easily seen by writing $\xi_1 = |\xi| \cos \phi$ and $\xi_2 = |\xi| \sin \phi$ which implies $(\xi_1^2 - \xi_2^2)/(\xi_1^2 + \xi_2^2) = \cos 2\phi$. Thus this factor does not have a well defined limit for $\xi_1 = \xi_2 = 0$ and is put equal to zero there, its average value with respect to ϕ . In the context of spectral accuracy as discussed above, a non regular function is a problem even if there is only one non-regular point since spectral methods are nonlocal.

Due to the absence of an explicitly known smooth periodic DS II solution, spectral convergence had not been tested in [13]. The D-bar approach to DS II allows one to address this issue. Using the direct solvers compared in [13], with data and computational parameters consistent with the example of Fig. 6, using $N_t = 10^4$ time steps, we find that the energy is conserved to the order of machine precision (the relative error between initial and final energy is $2\mathbf{e}-14$). The difference between this numerical solution and the one obtained with the D-bar code is of the order of 10^{-6} . This suggests that a regularization of the integrand in (97) along the lines developed in this paper for the D-bar problem will be beneficial also in the context of direct numerical approaches for DS II. A related approach will be discussed elsewhere.

Remark 6.1. One can also compare the performance of the D-bar solvers in sections 4 and 5 in the context of DS II solutions. Using the same parameters as above for both codes, the following table shows the L^∞ norm of the difference between both solutions. Specifically, we numerically solve the inverse problem, with predetermined reflection coefficient $r_0(k_1, k_2)e^{-\frac{it}{2}(\operatorname{Re}(k^2))}$, taking $t = 0.1$, in two ways: the only difference being in the way we computationally implement $\bar{\partial}^{-1}$, either using the method of Section 4 or the method described in this section (using the “shifting” described in Section 5). This indicates that the more economic code of section 4 can be used in this context if machine precision is not needed. The reason for the relatively

Fourier Modes	L	Error
2^6	2.25	7.3e-07
2^7	3.2	3.4e-09
2^8	4.2	5.2e-11

FIGURE 7. L^∞ norm of the difference between solution to DS-II at time $t = 0.8$ obtained via the D-bar approach in two ways: one way using the method of section 4 for the inversion of the D-bar operator, and one way using the method of section 5 for this inversion.

high accuracy of this code is that the biggest errors are introduced there for k and z close to the boundaries of the computational domains where the reflection coefficient and the solution are smallest. Thus these errors contribute comparatively little to the final result. But if the CGO solution of the D-bar problem is needed for values of k close to the boundary with high precision, the code of section 5 has to be used.

7. OUTLOOK

We have presented in this paper algorithms for the numerical computation of CGO solutions to D-bar problems. The presented approach is based on FFT techniques and a regularization of the functions submitted to FFTs via ϕ -functions. It was shown that the algorithms show spectral convergence and thus allow computations of the solution to the D-bar problem with essentially machine precision. The computational cost is mainly in two-dimensional FFTs which appear in an iterative resolution of the integral equation (81) via GMRES.

Whereas the convergence of the algorithm is as shown spectral, the solution of the equation (81) has to be computed for each considered value of k separately, which is time consuming. Thus a simple acceleration of the code on modern computers could be achieved by parallelizing the code in a way that the solution h is computed at the same time for several values of k . If higher resolutions than $N_x N_y > 2^{25}$ are needed, the corresponding FFTs are difficult to handle on a serial computer. Such resolutions can be necessary to study *dispersive shocks*, i.e., highly oscillatory regions of the DS II solution appearing in the *semiclassical* regime, see [12]. In this case a parallelization also of the two-dimensional FFTs is necessary as in [12]. The study of both types of parallelization will be the subject of further work.

The algorithms studied in the present paper are optimized for rapidly decreasing smooth functions. For algebraically decreasing functions and functions with compact support being just piecewise continuous, different techniques are necessary to obtain spectral convergence. Possible approaches are multi-domain spectral methods as in [3] and references therein, best after introducing special coordinates as polar coordinates. This will be studied in an ensuing publication.

ACKNOWLEDGEMENT

This work was supported in part by the Marie Curie IRSES program RIMMP. KM was supported in part by the National Science Foundation under grant DMS-1401268; he thanks the faculty and staff of the University of Burgundy for their hospitality during his stay as a visiting professor where part of this work has been completed, and for funding from the CNRS as a visiting researcher at the IMB. KM also thanks Robert Indik for sage advice and a number of helpful discussions.

REFERENCES

- [1] K. Astala, J. L. Mueller, L. Päiväranta, and S. Siltanen. Numerical computation of complex geometrical optics solutions to the conductivity equation. *Appl. Comput. Harmon. Anal.* **29**no. 1, 217 (2010).
- [2] K. Atkinson, An Introduction to Numerical Analysis (Wiley, second edition, 1989).
- [3] M. Birem and C. Klein, *Multidomain spectral method for Schrödinger equations*, arxiv.org/abs/1410.3718
- [4] R. M. Brown and G. Uhlmann. Uniqueness in the inverse conductivity problem for nonsmooth conductivities in two dimensions, *Comm. Partial Differential Equations* **22**, 1009 (1997).
- [5] Y. Chen. A fast, direct algorithm for the Lippmann-Schwinger integral equation in two dimensions, *Adv. Comp. Math.* **16**, 175 (2002).
- [6] D. Gilbarg, and N. S. Trudinger. *Elliptic Partial Differential Equations of Second Order*, Springer-Verlag, Berlin Heidelberg New York, 1977.

- [7] S. J. Hamilton, C. N. L. Herrera, J. L. Mueller, and A. Von Herrmann. A direct D-bar reconstruction algorithm for recovering a complex conductivity in 2-D. *Inverse Problems* **25**, 095005 (2012).
- [8] D. Isaacson, J. L. Mueller, J. C. Newell, and S. Siltanen. Imaging cardiac activity by the D-bar method for electrical impedance tomography. *Physiological Measurement* **27** S43-S50 (2006).
- [9] D. Isaacson, J. L. Mueller, J. C. Newell, and S. Siltanen. Reconstructions of chest phantoms by the D-bar method for Electrical Impedance Tomography. *IEEE Trans. on Med. Imaging* **23**, No. 7, 821-828 (2004).
- [10] P. Muller, D. Isaacson, J. Newell, and G. Saulnier. A Finite Difference Solver for the D-bar Equation. *Proceedings of the 15th International Conference on Biomedical Applications of Electrical Impedance Tomography, Gananoque, Canada—*, 2014.
- [11] A-K. Kassam and L.N. Trefethen. Fourth-Order Time-Stepping for stiff PDEs. *SIAM J. Sci. Comput.*, 26(4):1214–1233, 2005.
- [12] C. KLEIN AND K. ROIDOT, *Numerical Study of the semiclassical limit of the Davey-Stewartson II equations*, Nonlinearity **27**, 2177-2214 (2014).
- [13] C. KLEIN AND K. ROIDOT. Fourth order time-stepping for Kadomtsev-Petviashvili and Davey-Stewartson equations, *SIAM Journal on Scientific Computing* Vol. 33, No. 6, DOI: 10.1137/100816663 (2011).
- [14] S. Siltanen, J. L. Mueller, and D. Isaacson. An Implementation of the 2-D Reconstruction Algorithm of A. Nachman for the 2-D Inverse Conductivity Problem. *Inverse Problems* **16**, 681-699 (2000).
- [15] S. Siltanen, J. L. Mueller, and D. Isaacson. Reconstruction of High Contrast 2-D Conductivities by the Algorithm of A. Nachman. In AMS proceedings of the 2000 conference on Radon Transforms and Tomography, E. Quinto, editor, pp.241-254 (2001).
- [16] J. L. Mueller, S. Siltanen, and D. Isaacson. A direct reconstruction algorithm for electrical impedance tomography. *IEEE Trans. Med. Im.* **21**, 555 (2002).
- [17] K. Knudsen, M. Lassas, J. L. Mueller, and S. Siltanen. Regularized D-bar method for the inverse conductivity problem. *Inverse Problems and Imaging* **3**, 599-624 (2009).
- [18] K. Knudsen, J. L. Mueller, S. Siltanen. Numerical solution method for the d-bar equation in the plane. *J. Comput. Phys.* **198** no. 2, 500-517 (2004).
- [19] K. Knudsen. On the inverse conductivity problem, Ph.D. Thesis, Department of Mathematical Sciences, Aalborg University, Denmark, 2002.
- [20] V. Kolehmainen, M. Lassas, P. Ola, and S. Siltanen. Recovering boundary shape and conductivity in electrical impedance tomography. *Inverse Problems and Imaging* **7**(1), 217-242 (2013).
- [21] J.L. Mueller and S. Siltanen. *Linear and Nonlinear Inverse Problems with Practical Applications*, SIAM, 2012.
- [22] Y. Saad and M. Schultz, *GMRES: A generalized minimal residual algorithm for solving nonsymmetric linear systems*. *SIAM J. Sci. Comput.* **7** (1986), no. 3, 856–869.
- [23] G. Vainikko. Multidimensional weakly singular integral equations. *Lecture Notes in Mathematics* **1549**, Springer (1993).
- [24] A.I. Nachman. Global uniqueness for a two-dimensional inverse boundary value problem. *Ann. Math.* **143** (1996).
- [25] J.L. Mueller and S. Siltanen. Direct reconstructions of conductivities from boundary measurements. *SIAM J. Sci. Comput.* **24** p. 1232 (2003).
- [26] P. Perry. Global well-posedness and long-time asymptotics for the defocussing Davey-Stewartson II equation in $H^{1,1}(\mathbb{R}^2)$. Preprint available at arxiv.org/pdf/1110.5589v2.pdf.
- [27] L-Y Sung. An inverse scattering transform for the Davey-Stewartson II equations, I. *J. Math. Anal. and Appl.* **183**, 121-154 (1994).
- [28] P. White and J. Weideman, Numerical Simulation of Solitons and Dromions in the Davey-Stewartson System, *Math. Comput. Simul.*, **37** (1994), pp. 469-479.

(C. Klein) INSTITUT DE MATHÉMATIQUES DE BOURGOGNE 9 AVENUE ALAIN SAVARY, BP 47870, 21078 DIJON CEDEX
E-mail address: christian.klein@u-bourgogne.fr

(K. McLaughlin) DEPARTMENT OF MATHEMATICS, THE UNIVERSITY OF ARIZONA 617 N. SANTA RITA AVE. P.O. BOX 210089
 TUCSON, AZ 85721-0089 USA
E-mail address: mcl@math.arizona.edu